

# Discovery of $\delta$ Scuti pulsation in the Herbig Ae star VV Serpentis<sup>\*</sup>

V. Ripepi<sup>1</sup>, S. Bernabei<sup>2,3</sup>, M. Marconi<sup>1</sup>, A. Ruoppo<sup>1,4</sup>, F. Palla<sup>5</sup>, M. J. P. F. G. Monteiro<sup>6</sup>,  
J. P. Marques<sup>6</sup>, P. Ferrara<sup>1</sup>, S. Marinoni<sup>2</sup>, and L. Terranegra<sup>1</sup>

<sup>1</sup> INAF – Osservatorio Astronomico di Capodimonte, via Moiariello 16, 80131 Napoli, Italy  
e-mail: [ripepi;marconi;ruoppo;pferrara]@na.astro.it

<sup>2</sup> INAF – Osservatorio Astronomico di Bologna, via Ranzani 1, 40127 Bologna, Italy  
e-mail: stefano.bernabei@bo.astro.it; silvia.marinoni@bo.astro.it

<sup>3</sup> Departamento de Astrofísica, Universidad de La Laguna, Avda. Astrofísico F. Sánchez sn, 30071 La Laguna, Spain

<sup>4</sup> Dipartimento di Scienze Fisiche, Università Federico II, Complesso Monte S. Angelo, 80126 Napoli, Italy

<sup>5</sup> INAF – Osservatorio Astrofisico di Arcetri, Largo E. Fermi 5, 50125 Firenze, Italy  
e-mail: palla@arcetri.astro.it

<sup>6</sup> DMA-Faculdade de Ciências and Centro de Astrofísica da Universidade do Porto, Rua das Estrelas, 4150-762 Porto, Portugal  
e-mail: mjm@astro.up.pt

Received 31 May 2006 / Accepted 2 October 2006

## ABSTRACT

**Context.** The study of pulsation in pre-main-sequence intermediate mass stars represents an important tool for deriving information on the stellar parameters and structure, as well as for testing the validity of current theoretical models. The interest in this class of variable stars has significantly increased during the last decade and about 30 members are presently known in the literature.

**Aims.** A new observational study of the Herbig Ae star VV Ser has been performed to detect and accurately measure pulsation frequencies in the  $\delta$  Scuti range, thus enlarging the sample of known pulsators and contributing to the empirical definition of the pre-main-sequence instability strip. As it belongs to the continuous field of view of the asteroseismological satellite COROT, this study also aims at characterizing the properties of VV Ser as a potential “COROT additional program” candidate.

**Methods.** CCD time series photometry in the Johnson *V* filter has been obtained for three consecutive years. The resulting light curves have been subject to detailed frequency analysis and the derived frequencies have been compared to model predictions.

**Results.** Seven pulsation frequencies have been measured on the basis of the best data set obtained in 2004, ranging from  $\sim 31$  to  $\sim 118$   $\mu$ Hz, with an accuracy of the order of 0.5  $\mu$ Hz. The comparison with an extensive set of asteroseismological models shows that all the observed periodicities can be reproduced if the stellar mass is close to 4  $M_{\odot}$ . Conversely, the measured frequencies can be associated with *p* modes only if the effective temperature is significantly lower than that obtained from the spectral type conversion.

**Conclusions.** The present results seem to suggest that more accurate spectral type determination is necessary to discriminate the best-fit model solution. In any case, the stellar mass of VV Ser is close to the upper mass limit ( $\sim 4 M_{\odot}$ ) for this class of pulsators.

**Key words.** stars: variables:  $\delta$  Scuti – stars: oscillations – stars: pre-main sequence – stars: fundamental parameters – stars: individual: VV Serpentis

## 1. Introduction

Pre-main-sequence (PMS) stars with masses larger than 1.5  $M_{\odot}$  are known as Herbig Ae/Be stars (Herbig 1960). In general, they are found within star-forming regions and show variable emission lines (especially  $H\alpha$ ), as well as strong infrared excess caused by the presence of circumstellar material (dust). In addition, Herbig Ae/Be stars are characterized by photometric and spectroscopic variability on timescales of minutes to years, mainly due to photospheric activity and interaction with the circumstellar environment (see, e.g., Gahm et al. 1995; Böhm & Catala 1995).

Considerable theoretical work has been done recently that has advanced our understanding of PMS evolution (e.g., Palla & Stahler 1993; D’Antona & Mazzitelli 1994; Swenson et al. 1994). Yet, there remain differences in the models owing to alternative treatments of convection, opacities, and the zero-point of the calculated ages. It is therefore desirable to

find independent tools to constrain PMS evolutionary tracks and, in turn, the internal structure of intermediate-mass PMS stars.

Asteroseismology of Herbig Ae/Be stars can in principle allow us to test PMS models by probing their interiors. It is now well established that intermediate-mass PMS stars during their contraction towards the MS cross the pulsation instability strip of more evolved stars, giving origin to a variable class named PMS  $\delta$  Scuti stars (Kurtz & Marang 1995; Marconi & Palla 1998; Catala 2003; Ripepi et al. 2006a). The existence of pulsating Herbig Ae stars was originally proposed by Breger (1972), who discovered two candidates in the young open cluster NGC 2264. More than 20 years later, the suggestion was confirmed by Kurtz & Marang (1995) and Donati et al. (1997), who observed  $\delta$  Scuti-like pulsations in the Herbig Ae stars HR 5999 and HD 104237, respectively.

The first theoretical investigation of the PMS instability strip based on non-linear convective hydrodynamical models was carried out by Marconi & Palla (1998), who calculated its topology for the first three radial modes. A subsequent theoretical work by Suran et al. (2001) made a comparative study of the seismology

<sup>\*</sup> Tables 3, 5 and 6 are only available in electronic form at <http://www.aanda.org>

of a  $1.8 M_{\odot}$  PMS and post-MS star. Suran et al. (2001) found that the unstable frequency range is roughly the same for PMS and post-MS stars, but that some nonradial modes are very sensitive to the deep internal structure. In particular, it is possible to discriminate between the PMS and post-MS phase using differences in the oscillation frequency distribution in the low frequency range ( $g$  modes).

Since the work by Marconi & Palla (1998), many new PMS  $\delta$  Scuti candidates have been observed and the current number of known or suspected candidates amounts to about 30 stars (see, e.g., Zwintz et al. 2004; Ripepi et al. 2006a). However, only a few stars have been studied in detail (e.g., Ripepi et al. 2003; Böhm et al. 2004; Ripepi et al. 2006b), so that the overall properties of this class of variables are still poorly determined. In this context, our group started a systematic photometric monitoring program of Herbig Ae stars with spectral types from A to F2-3 in the year 2000 (see, e.g., Marconi et al. 2000; Ripepi et al. 2002; Pinheiro et al. 2003; Ripepi et al. 2003; Ripepi et al. 2006b). The aims were: 1) to identify observationally the boundaries of the instability strip for PMS  $\delta$  Scuti pulsation; 2) to study in detail selected objects showing multiperiodicity through multisite campaigns. As part of this long-term project, we present a new observational study devoted to the Herbig Ae star VV Ser here. In addition to the motivation mentioned above, this star conveniently falls in the continuous field of view of the asteroseismological satellite COROT (corot.oamp.fr). Thus, VV Ser represents a potential “additional program” candidate (Weiss et al. 2004).

In the next section, we discuss the properties of VV Ser; in Sect. 3 we describe the observations and data reduction; in Sect. 4 we deal with the frequency analysis; in Sect. 5 we present a comparison with theoretical predictions. Finally, a brief summary closes the paper.

## 2. Stellar parameters of VV Ser

The variable star VV Ser was identified as a young Ae star in the seminal work by Herbig (1960) on emission line stars associated with reflection nebulae. The star is located in the Serpens molecular cloud (Chavarría et al. 1988) and has been widely studied in literature, although its properties and position in the HR diagram are still rather uncertain. In the following, we present an overview of the current observational status of VV Ser.

- **Spectral type and luminosity class:** we report all the independent measurements of spectral type (ST) found in the literature in Table 1 (first column). The uncertainty is large with ST varying between B1e-B3e and A3e. The determination of the earliest type by Finkenzeller & Mundt (1984) is based on the HeI 5876 Å line, which was later found to be associated with the hot regions of accretion disks (see Rostopchina et al. 2001, and references therein) and therefore should not be considered reliable. However, a B5–B9 type has also been claimed by other authors (see Table 1). On the other hand, Table 1 lists six studies where VV Ser is classified as an Ae star, with typical value A2. Interestingly, the only paper exclusively dedicated to VV Ser is that by Chavarría et al. (1988), who assigns an A2e class, based on high resolution spectroscopy and Strömgren photometry. In the following, we will rely on these results, allowing an uncertainty of 2 subclasses to take into account the spread of spectral types found in the literature. Concerning the luminosity class of VV Ser, there are three determinations in the literature: class II (Gray & Corbally 1998),

**Table 1.** Literature values of spectral type, luminosity class, and rotational velocities for VV Ser.

Sp. type	$v \sin i$ km s <sup>-1</sup>	Source
A2e		Herbig (1960)
A:		Cohen & Kuhl (1979)
B1e-B3e		Finkenzeller & Mundt (1984)
A2eV $\beta$		Chavarría et al. (1988)
B9e <sup>1</sup>	200 <sup>2</sup>	Hillenbrand et al. (1992)
B5e		Fernández et al. (1995)
	85 <sup>3</sup>	Grady et al. (1996)
A3IIe $\beta$		Gray & Corbally (1998)
A0Vep <sup>4</sup>	229 $\pm$ 9 <sup>5</sup>	Mora et al. (2001)
B+sh	142	Vieira et al. (2003)
A2IIIe <sup>6</sup>		Acke & van den Ancker (2004)
B6e		Hernández et al. (2004)

<sup>1</sup> Photometrically determined; <sup>2</sup> no reference is indicated for this value; <sup>3</sup> the authors quote Hillenbrand et al. (1995, private communication) as the source for this value; <sup>4</sup> the authors quote an error of five classes; <sup>5</sup>  $v \sin i$  derived using just one line (MgII 4481 Å line); <sup>6</sup> the authors quote van den Ancker (private communication) as the source for this value.

III (Acke & van den Ancker 2004), and V (Mora et al. 2001). Again, there is no agreement between different authors.

- **Distance and position in the HR diagram:** the distance estimate of VV Ser is related to that of the Serpens Cloud. On the basis of photometric and spectroscopic observations of 5 stars in the cloud (excluding VV Ser), Chavarría et al. (1988) and de Lara et al. (1991) calculated a distance of  $D = 311 \pm 38$  pc, in fair agreement with previous determinations of about 440 pc by Racine (1968) and Strom (1974). In the following, we will adopt a distance of 300–400 pc. As for the position in the HR diagram, Table 2 lists several estimates of  $\log(T_{\text{eff}})$  and  $\log(L/L_{\odot})$  found in the literature. The table highlights the existing uncertainties, mainly because of different assumptions on the ST, on the visual absorption, and on the apparent visual magnitude of VV Ser, which varies by a tenth of magnitude on timescales of weeks.
- **Rotational velocity:** another source of uncertainty in the analysis of VV Ser is represented by its rotational velocity. Table 1 reports four independent measurements of  $v \sin i$  found in the literature. The values reported by Hillenbrand et al. (1992) and Mora et al. (2001) are in fair agreement, whereas those given by Grady et al. (1996) and Vieira et al. (2003) are significantly different. More specifically, we were not able to find the source of the  $v \sin i$  reported by Hillenbrand et al. (1992), who quoted the studies of Finkenzeller (1985) and Davis et al. (1983) that, however, do not give a value for VV Ser. Similarly, the low  $v \sin i$  reported by Gray & Corbally (1998) cannot be verified because it is quoted as private communication. Finally, the  $v \sin i$  measured by Mora et al. (2001) is somewhat uncertain because it relies on just one line, the MgII 4481 Å line. Thus, the rotational velocity of VV Ser is still uncertain, even if there are indications that it could be larger than 100 km s<sup>-1</sup>. This possibility will be taken into account in the interpretation of the data (see Sect. 5).

In conclusion, the empirical estimate of the stellar parameters of VV Ser is still plagued by large errors. However, as we will discuss in Sect. 5, the pulsational analysis of the detected

**Table 2.** Stellar parameters for VV Ser found in the literature.

$V$ mag	$D$ pc	$A_V$ mag	$\log(T_{\text{eff}})$ K	$\log(L)$ $L_{\odot}$	$M$ $M_{\odot}$	Source
12.666	245	6.1	3.95	>1.62		1
11.87	440	3.0	4.03	1.8	3.3	2
11.92	440	3.4	4.14	2.23	3.8	3
11.63	296	3.4	3.95	1.51	2.1	4
11.58	440		4.03	2.03		5
	330	2.7	3.95	1.27		6

<sup>1</sup> Chavarría et al. (1988); <sup>2</sup> Hillenbrand et al. (1992); <sup>3</sup> Hernández et al. (2004); <sup>4</sup> Rostopchina et al. (2001); <sup>5</sup> Testi et al. (1998); <sup>6</sup> Acke & van den Ancker (2004).

frequencies can help to reduce the uncertainty on luminosity, effective temperature, and mass.

### 3. Observations and data reduction

The observations of VV Ser have been carried out in several runs during 2002, 2003, and 2004 (a detailed observational log is given in electronic form in Table 3), using the Loiano 1.5 m telescope equipped with the BFOSC instrument (see <http://www.bo.astro.it/loiano/index.htm> for a detailed description of the telescope and of the instruments). The CCD is a EEV 1340  $\times$  1300 pixels with individual size of 0.58 arcsec, for a total field of view of 13'  $\times$  13'. In total, about 55 h of observations have been gathered in the Johnson  $V$  filter. The comparison star used was USNO-A2.0 0900-12930815 (18<sup>h</sup>28<sup>m</sup>33.535<sup>s</sup> +00°02'25.71"J2000), which is about 7.3<sup>m</sup> away from VV Ser, allowing us to observe both stars in a single BFOSC frame. We note that this star has already been used as a comparison for VV Ser by Fernández (1995), who found it stable at a level of 0.02 mag and with an apparent magnitude and color of  $V = 12.28$  mag ( $B - V = 0.89$  mag, respectively).

All the data have been reduced following the usual procedures (de-biasing, flat-fielding) by using standard IRAF routines. The aperture photometry has been carried out using routines written in the MIDAS environment. The typical precision of the data was of about 4, 6, and 3 mmag for the 2002, 2003, and 2004 data sets, respectively. On this basis (see also Figs. 1 and 2) it is evident that the 2002 and especially the 2004 data sets are the best ones, whereas the 2003 run is of poor quality. Note that, because of the high sampling, the 2004 data have been smoothed by using a 3-point boxcar filter.

The observed light curves for the different data sets are reported in Fig. 1. It is evident that VV Ser displays mid-term variations on timescales of days, in addition to the pulsation on timescales of hours. To eliminate these night-to-night variations and to prepare the data for Fourier analysis, we decided to detrend the data to a common average zero value. Then, we used the period04 package (Lenz & Breger 2005) to remove the frequencies 0.60 c/d from the 2002 data set, 0.46 c/d+0.19 c/d from the 2003 data set, and 0.45 c/d from the 2004 data set, with the exception of the two nights with HJD = 53 209 and 53 210 for which a simple average was subtracted. As a result, in Fig. 2 we show the light curves for the three data sets after the detrending procedure.

Before proceeding with the frequency analysis of the obtained time series, we would like to discuss more in detail the mid-term light variations with period of the order of 2 d, which

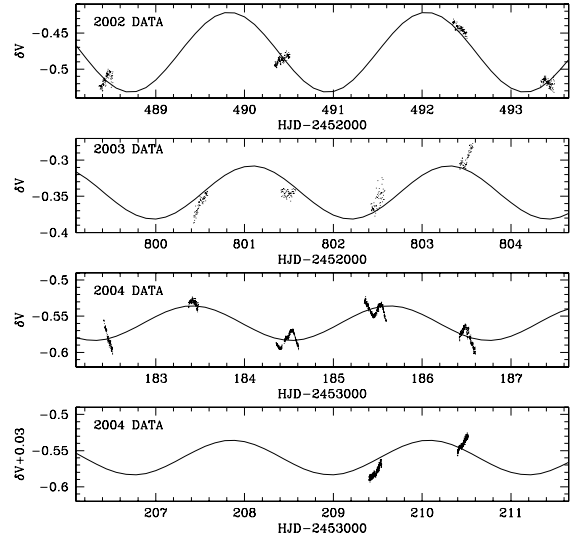


**Fig. 1.** From top to bottom, the first two panels show the 2002 and 2003 data set; the third and fourth panels show the 2004 data sets. Note that in the latter we have added 0.03 mag to the original differential photometry (see Sect. 3). The solid line shows the fit with a sin curve with a fixed period of 2.2 d and free amplitude and phase (for each data set, see Sect. 3).

have been removed from the data as described before. To investigate this point further, we fitted a sinusoid with the period  $P = 2.2$  d (frequency 0.45 c/d) found using the 2004 data (HJD = 53 182–53 186) for the three data sets, leaving the amplitude and phases as free parameters (to this end we added 0.03 mag to the photometry obtained during the nights with HJD = 53 209 and 53 210). The result is shown in Fig. 1 by a solid line: the fit is fairly good also for the 2002 data set, whereas it is worse for the 2003 data set. In conclusion, a periodicity of the order of 2 d seems to be present in VV Ser. It is worth noticing that analyzing six year data, Shevchenko et al. (1993) found both a long-term periodicity (around 1000 d) and a short-term periodicity (which they quote as uncertain) of 3.9 d. Even if there is a discrepancy between Shevchenko et al. (1993)'s results and ours, the short-term periodicity could be real. The physical origin of this kind of periodicity is not easily understood and in any case is not the subject of this paper. However, such short-term variability in Herbig Ae stars is generally attributed to rotational modulation due to magnetic activity (see, e.g., Catala et al. 1999).

### 4. Frequency analysis

The detrended time series shown in Fig. 2 have been analyzed using the period04 package (Lenz & Breger 2005), based on the Fourier transform method, again. For a better interpretation of the results, we first calculated the spectral window (SW) for each data set. The result is shown in Fig. 3, where from top to bottom we report the SW for the three time series identified in the previous section (see labels in the figure). The SW was used as a diagnostic to distinguish between real and spurious frequencies.

Each data set described in the previous section has been analyzed separately. Figure 4 (left panels) shows the Fourier transform for the 2002 and 2003 data sets, whereas Fig. 4 (right panels) displays the 2004 one. Here, in each panel the peak with largest amplitude is selected and then removed, obtaining a new spectrum shown in the next panel. The last panel shows the periodogram after the prewhitening with all the significant

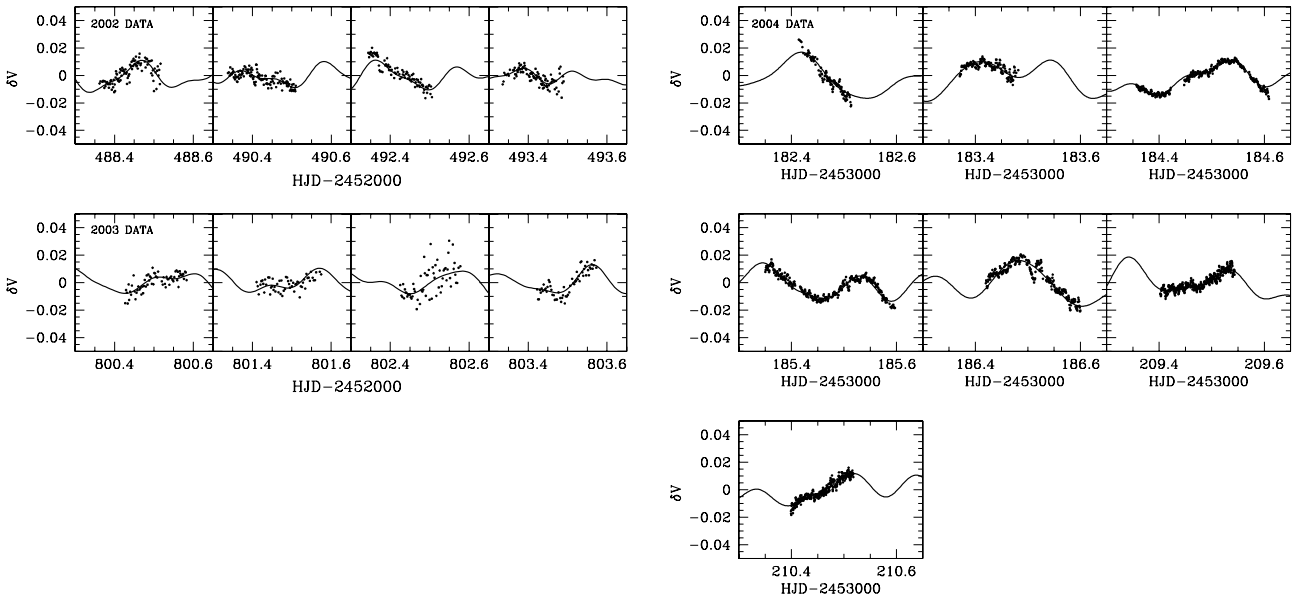


**Fig. 2.** *Left panels:* light curves for the 2002 (*top*) and 2003 (*bottom*) data sets after the detrending. Note that  $\delta V = V_{\text{VAR}} - V_{\text{COMP}}$ . *Right panels:* as before, but for the 2004 data set. In all the panels, the solid line displays the fit to the data with all the significant frequencies found for each data set, as listed in Table 4.

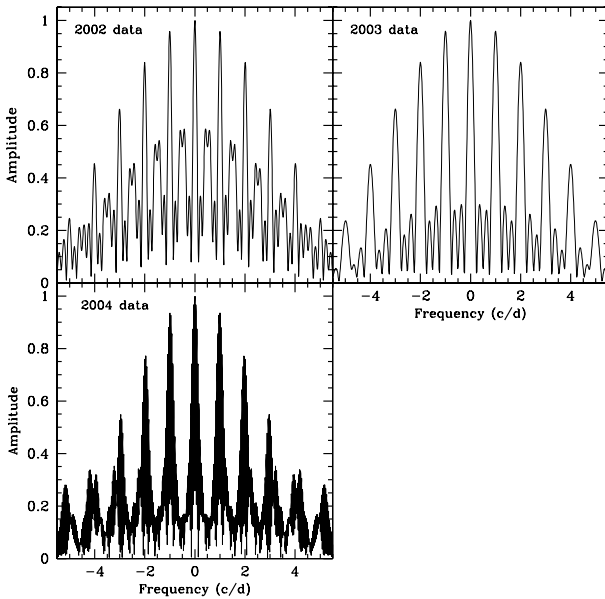


**Fig. 3.** Spectral window in amplitude for the three data sets analyzed in this paper (see labels in the figure).

frequencies. The different lines represent the 99.9%, 99%, and 90% confidence levels calculated following the widely used recipe by Breger et al. (1993) and Kuschnig et al. (1997). The error on the measured frequencies (apart from the  $\pm 1$  c/d alias) can be roughly estimated from the FWHM of the main lobe in the spectral window (see Alvarez et al. 1998 and references therein). As a result, we found  $\Delta f \sim 0.14$  c/d,  $0.22$  c/d, and  $0.04$  c/d for the 2002, 2003, and 2004 data sets. For the last data set, due to the complex structure of the main lobe of the spectral window, to be conservative, we doubled the nominal error. It is important to emphasize that all the frequencies reported in the following are affected by the indetermination due to the 1 c/d alias.

All the significant frequencies found for the three data sets are summarized in Table 4. A fit to each data set with the quoted frequencies is shown in Fig. 2 by a solid line.

To discuss the results of the frequency analysis in detail, we will take the frequencies obtained with the best data set, that of 2004, as reference. Then, we find:

- $f_1 = 6.12$  c/d: it is found in all data sets within the quoted errors. The first frequency in 2002 is clearly the  $-1$  c/d alias (this periodicity also has the same amplitude as in 2004), whereas in 2003 it has a significantly lower amplitude, owing to the poor quality of the data set and/or to a possible change in amplitude (common occurrence among  $\delta$  Scuti stars);
- $f_2, f_3, f_6, f_7$ : they have only been found in the 2004 data set. We note that  $f_7$  would be exactly twice  $f_1$  if we took the  $-1$  c/d alias; therefore, it could be a non-independent frequency. Moreover, it is only partially significant (90%);
- $f_4 = 3.90$  c/d: within the errors, it can be considered the same frequency as in the 2002 ( $f_4 = 3.84$  c/d) and 2003 ( $f_4 = 3.99$  c/d) data sets;
- $f_5 = 9.96$  c/d: it could correspond to the frequencies at  $9.55$  c/d and  $8.50$  c/d ( $-1$  c/d alias) in the 2002 and 2003 data sets. Although these three frequencies are not equivalent within the errors, we will assume that they represent the same frequency because of the similar amplitudes.

In the following, we will use the set of 6 significant frequencies extracted from the 2004 data set for comparison with theoretical models.

## 5. Comparison with theory

We now attempt to use the frequency data reported above to carry out a preliminary comparison of the available observables with theoretical models. To do so, we consider the observed location of the star in the theoretical HR diagram and how a tentative mode identification of the observed frequencies can

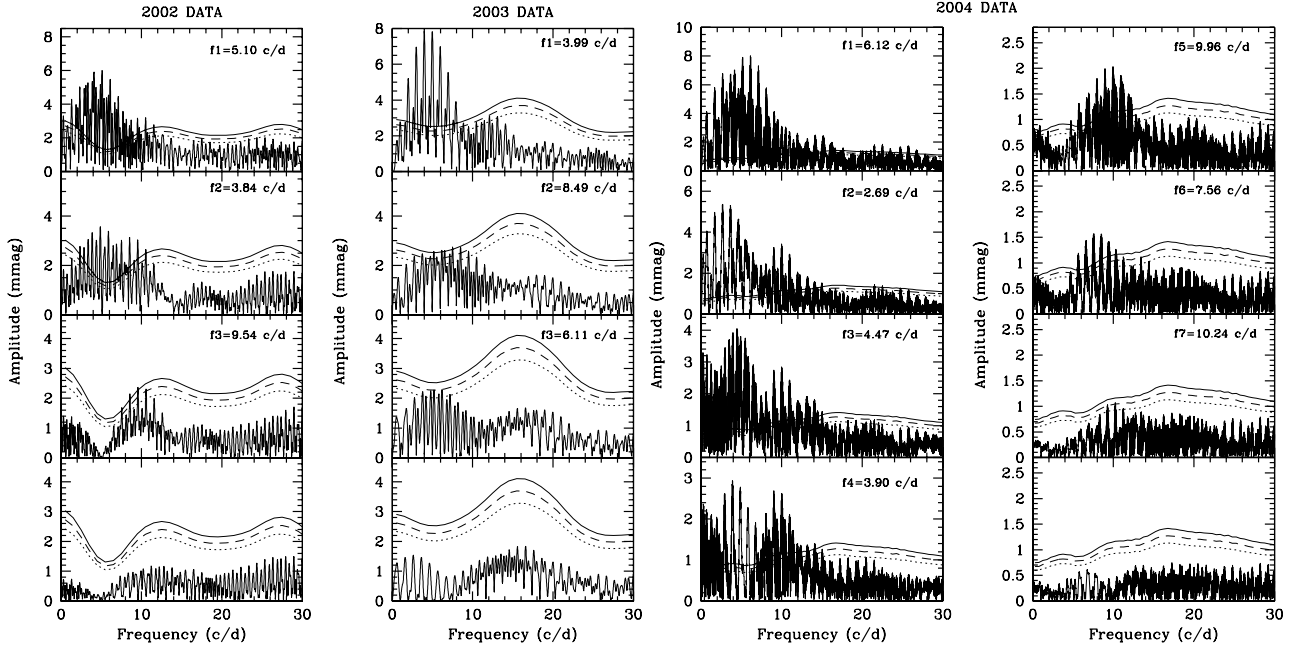


**Fig. 4.** *Left panels:* frequency analysis for the 2002 and 2003 data sets. The solid, dashed, and dotted lines show the 99.9%, 99%, and 90% significant levels. In each panel, one peak (i.e. the labeled frequency) is selected and removed from the time series and a new spectrum is obtained. The last panel displays the periodogram after the prewhitening with all the significant frequencies. *Right panels:* as before, but for the 2004 data set.

**Table 4.** Frequencies, amplitudes, and confidence levels for the three data sets analyzed in this paper. The errors on the 2002, 2003, and 2004 data are  $\sim 0.14$  c/d,  $\sim 0.22$  c/d, and  $\sim 0.04$  c/d, respectively. Note that for the 2002 and 2003 data sets, the frequencies are labeled in correspondence to the 2004 data set (see text).

	Frequency (c/d)	Amplitude (mmag)	Confidence (%)
2002 DATA			
$f_1$	5.11	6.3	99.9
$f_4$	3.84	4.6	99.9
$f_5$	9.55	2.9	99.9
2003 DATA			
$f_4$	3.99	7.6	99.9
$f_5$	8.50	2.3	99.0
$f_1$	6.11	3.1	90.0
2004 DATA			
$f_1$	6.12	6.4	99.9
$f_2$	2.69	7.8	99.9
$f_3$	4.47	3.7	99.9
$f_4$	3.90	4.8	99.9
$f_5$	9.96	2.7	99.9
$f_6$	7.56	2.1	99.9
$f_7$	10.24	1.4	90.0

constrain the stellar mass. Because the outcome depends strongly on the assumptions, we will also evaluate the effects of the uncertainties on the results.

### 5.1. Location in the HR diagram

To compare the observations with the theoretical predictions, it is necessary to estimate the position of VV Ser in the HR diagram. As discussed in Sect. 2, spectral type and distance to VV Ser are quite uncertain. First, we have estimated the  $T_{\text{eff}}$

value from the adopted spectral type  $A2 \pm 2$  subclass by using the Schmidt-Kaler (1965) conversion tables, noting that for these relatively early-types these values are in agreement with the more recent estimates of, e.g., Kenyon & Hartmann (1995) (see their Table A5). As a result, we obtain  $T_{\text{eff}} = 9000 \pm 1000$  K. Concerning the luminosity, we decided to investigate all the values in the range  $1.3 < \log L/L_{\odot} < 2.3$ , covering the empirical estimates in the literature. The studied region is represented by the large box in the HR diagram shown in Fig. 5 that includes a set of PMS evolutionary tracks computed using the CESAM code (Morel 1997; Marques et al. 2004) for stellar masses from 1.5 to  $4.5 M_{\odot}$ , and the theoretical instability strip computed for the first three radial modes by Marconi & Palla (1998), on the basis of nonlinear convective pulsation models. We note that for the estimated effective temperatures of VV Ser, we do not expect pulsation in the first three radial modes since the predicted instability strip is cooler at each luminosity level. We might instead expect pulsation in higher radial overtones and/or in non-radial modes. In fact the instability strip is predicted to move toward higher effective temperatures as the radial overtone increases (see Grigahcène et al. 2006).

### 5.2. Oscillation frequencies

To evaluate the sensitivity of the predicted periodicities to the input stellar parameters, we computed a fine grid of structure models along the CESAM evolutionary tracks covering a mass range from 2.2 to  $4.0 M_{\odot}$  and effective temperatures from  $\sim 8000$  K to  $\sim 10000$  K. The physical properties of the selected PMS models are reported in Table 5 (available in electronic form). For each model, frequencies for  $l = 0, 1, 2^1$  modes were computed using the Aarhus adiabatic nonradial pulsation code

<sup>1</sup> The reason why we consider only  $l = 0, 1, 2$  modes is that, as noticed by other authors (see, e.g., Suran et al. 2001; Baglin et al. 2000), these modes are expected to be easily detectable, as their visibility coefficients remain large after integration over the whole stellar disk.

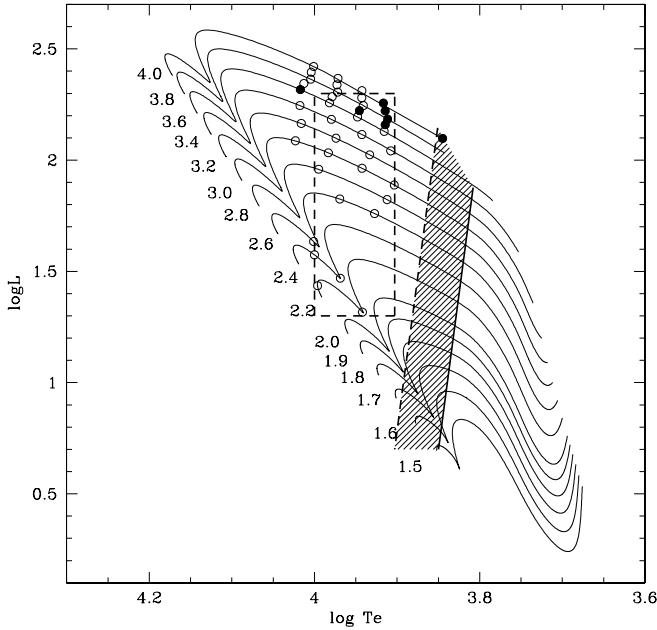


**Fig. 5.** PMS evolutionary tracks for the labeled masses and solar chemical composition ( $Z = 0.02$ ,  $Y = 0.28$ ) computed with the CESAM code. The dashed box represents the estimated uncertainty on the position of VV Ser. It is also shown the location of the theoretical instability strip for the first three radial modes predicted by Marconi & Pallà (1998) on the basis of nonlinear convective pulsation models. The empty circles represent the 32 models run for the pulsational analysis. The filled symbols are for the best-fit models discussed in Sect. 5.

(ADPLS-<http://astro.phys.au.dk/~jcd/adipack.n/>) and compared with the observed periodicities. The range covered by the predicted frequencies depends on both the stellar mass and the effective temperature, moving toward higher values as the stellar mass (effective temperature) decreases (increases) at fixed effective temperatures (mass). In Figs. 6–9 the predicted frequencies with  $l = 0$ ,  $l = 1$ , and  $l = 2$  are compared with the empirical periodicities (labeled horizontal solid lines) for the labeled masses and effective temperatures.

We find that the three lowest frequencies, namely  $f_2$ ,  $f_3$ , and  $f_4$ , cannot be reproduced simultaneously by  $p$  modes in the explored mass and effective temperature range. In particular,  $f_2$  is only consistent with a  $g$  mode ( $l = 1, 2$  with  $n < 0$ ) unless the effective temperature is much lower than the estimated empirical range. To illustrate this point, we show the plot for a significantly cooler model ( $T_{\text{eff}} = 6997$  K) with  $M = 4.0 M_{\odot}$  in the left bottom panel of Fig. 9. In this case, the range of the three lowest observed frequencies is covered with the predicted  $l = 0$ ,  $n = 0, 1, 2$  modes, with  $f_2$  close to the theoretical result for the fundamental mode. Pulsation in these low order radial modes at such a low effective temperature is also expected on the basis of the location of the predicted instability strip (see Fig. 5).

A tentative mode identification based on the various plots is summarized in Table 6, available in electronic form. Model frequencies are required to match the observed ones within  $2.5 \mu\text{Hz}$ , to take into account both the mean error on the measured periodicities ( $\sim 0.5 \mu\text{Hz}$ ) and an estimate of the (unknown) model intrinsic uncertainty. The models reproducing all the observed frequencies with  $l = 0, 1, 2$   $p$  and/or  $g$  (or  $f$ ) modes are the ones reported in Table 7 and shown in Fig. 5. The stellar mass and luminosity associated with these models range from  $3.6$  to  $4.0 M_{\odot}$  and from  $125.2$  to  $207.6 L_{\odot}$ . To remove the degeneracy on the model solution, an independent empirical estimate of the

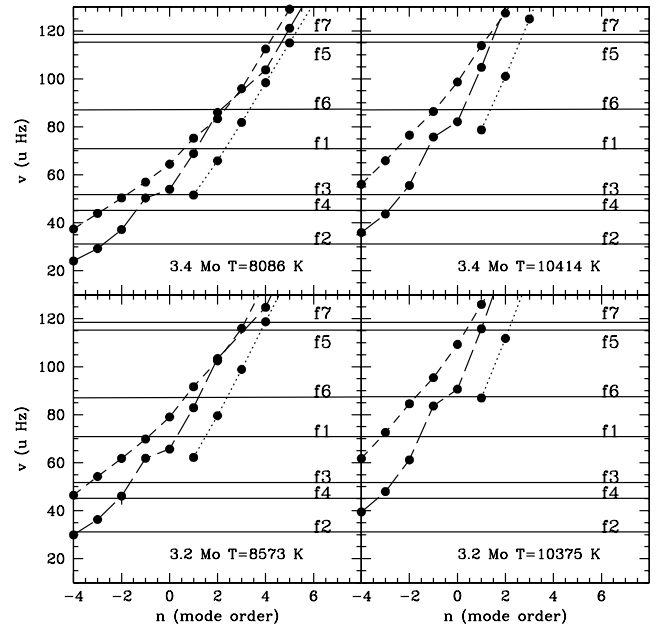


**Fig. 6.** Comparison between predicted (filled symbols) and observed (horizontal solid lines) periodicities for models at  $3.2 M_{\odot}$  (bottom panels) and  $3.4 M_{\odot}$  (upper panels). Symbols are connected by a dotted line for  $l = 0$ , by a long-dashed line for  $l = 1$ , and by a dashed line for  $l = 2$ . The two panels refer to the labeled effective temperatures. When a predicted frequency reproduces an observed one the corresponding filled symbol (along the given  $l$  slanting line) is located at the intersection with the horizontal line representing the observed value.

large separation would be very important. However, the evaluation of the large separation from the frequency power spectrum would require more accurate, long-time data.

We note that, among the best-fit models, mod37 is inside the theoretical instability strip for the three lowest radial modes, so that  $f_2$  and  $f_3$  are correctly reproduced by pulsation in the fundamental and the second overtone, respectively. In this case all seven observed frequencies can indeed be reproduced by  $p$  modes. Therefore, the results seem to suggest that either the effective temperature found in the literature is significantly overestimated, or that we have to admit the possibility of pulsation in at least one  $g$  mode.

Available studies point towards the existence of unstable low degree  $p$ -modes in PMS stars. Consequently, in the above analysis, models with  $p$ -modes in the observed frequency range have been preferred. The possibility that  $g$ -modes are also excited to the observed amplitudes has yet to be confirmed by a detailed theoretical analysis of the excitation mechanisms of such modes in young stars and supported by observational mode identification. A more detailed analysis (theoretical and observational) in this direction is clearly required.

### 5.3. Effect of rotation on mode identification

Here, we give a simplified, preliminary account of the effect of rotation on nonradial modes using the asymptotic relation for the rotational displacement. This is given by  $m f_{\text{rot}}$ , where  $m$  is the spherical harmonic number and  $f_{\text{rot}} = (v_{\text{rot}} \sin i) / (2\pi R \sin i)$  the rotational frequency. The term  $v_{\text{rot}} \sin i$  can be taken from published values. According to Sect. 3, the rotational velocity varies between a minimum of  $v_{\text{rot}} \sin i \sim 85 \text{ km s}^{-1}$  and a maximum of  $200 \text{ km s}^{-1}$ . For the  $\sin i$  term in the denominator,

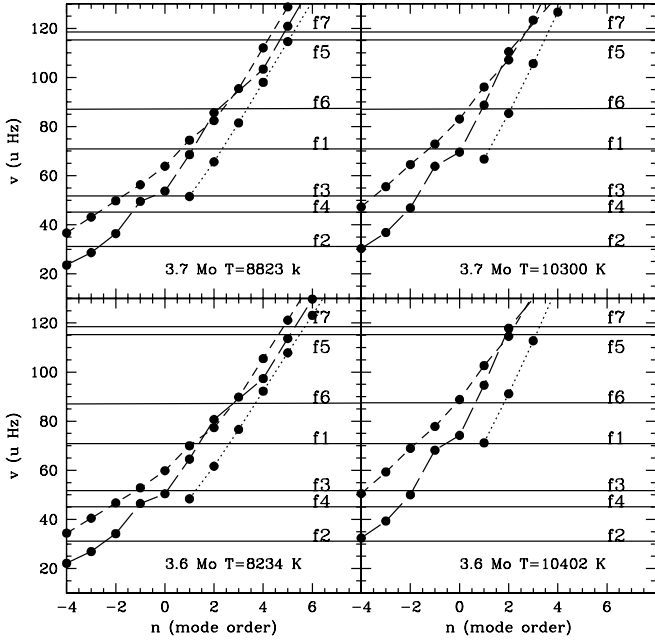


**Fig. 7.** The same as for Fig. 6, but for  $3.6 M_{\odot}$  (bottom panels) and  $3.7 M_{\odot}$  (upper panels).

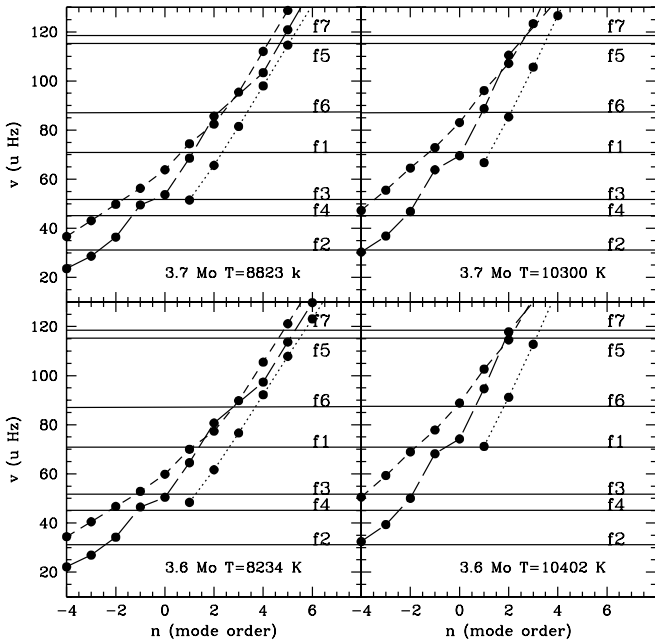


**Fig. 8.** The same as for Fig. 6, but for  $3.8 M_{\odot}$  (bottom panels) and  $3.9 M_{\odot}$  (upper panels).

we need to make an assumption on the inclination angle  $i$ . For simplicity, we consider two extreme cases, namely  $i_1 = \pi/4$  and  $i_2 = \pi/2$ . Finally, for the theoretical radius we take the values of our best-fit models as given in Table 7. Adopting  $v_{\text{rot}} \sin i = 200 \text{ km s}^{-1}$ , we find a rotational splitting  $8.5(17) \leq \Delta f_1 \leq 14.6(29.2) \mu\text{Hz}$  and  $6(12) \leq \Delta f_2 \leq 10.3(20.6) \mu\text{Hz}$  for  $m = \pm 1(2)$ , respectively. Conversely, for a velocity of  $85 \text{ km s}^{-1}$  the splittings are reduced to  $3.6(7.2) \leq \Delta f_1 \leq 6.2(12.4) \mu\text{Hz}$  and  $2.5(5.0) \leq \Delta f_2 \leq 4.4(8.8) \mu\text{Hz}$  for  $m = \pm 1(2)$ , respectively. We have also calculated the upper limit of  $\Delta f$  under the extreme assumption of  $v < v_{\text{breakup}}$ , where  $v_{\text{breakup}}$  is the break up velocity for the models reported in Table 7, yielding  $\Delta f_{\text{max}} \sim 20 \mu\text{Hz}$

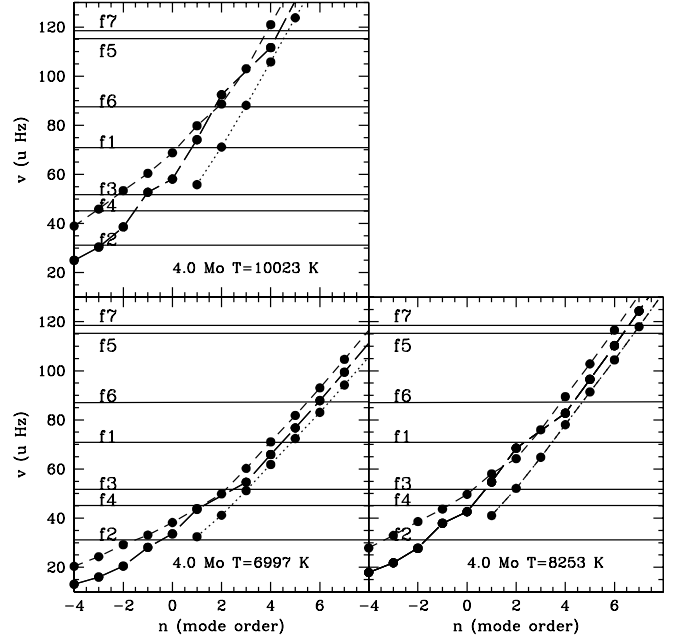


**Fig. 9.** The same as for Fig. 6, but for  $4 M_{\odot}$ .

and thus suggesting that the rotational splitting might introduce significant error bars on the theoretical mode identification.

On the other hand, if we assume that the measured periodicity at 2.2 d is associated with rotation, we derive a rotational splitting of  $\approx \pm 5(10) \mu\text{Hz}$  for  $m = \pm 1(2)$ , in better agreement with the values  $m \times 2.5$  to  $m \times 4.4 \mu\text{Hz}$  obtained for a rotational velocity of  $85 \text{ km s}^{-1}$  and a radius range covered by the best-fit models reported in Table 7 and a star seen close to edge-on ( $i = \pi/2$ ). Thus, these initial results seem to indicate that rotation may significantly affect the theoretical mode identification, with larger radii providing smaller rotational splitting for a given rotational velocity. However, since rotation alters the structural and evolutionary properties of stellar models, an accurate estimate of the effects on mode identification can only be obtained by a specifically designed numerical code that incorporates all the relevant physical ingredients (see, e.g., Reese et al. 2006).

## 6. Conclusions

We have detected  $\delta$  Scuti-type pulsation in the Herbig Ae star VV Ser on the basis of ground-based observations carried out during three consecutive years. In particular, using the best data set obtained in 2004, seven pulsation frequencies have been measured with values ranging from 2.69 to 10.24 c/d. These results allow us to include VV Ser in the list of known PMS stars with  $\delta$  Scuti variations (Zwintz et al. 2004; Ripepi et al. 2006a). To compare the extracted periodicities with model predictions, we have considered a large empirical range both in luminosity and effective temperature, reflecting the existing uncertainties on the stellar properties. Within this space of physical parameters, we have computed a fine grid of inner structure models along the CESAM evolutionary tracks. The corresponding pulsation frequencies for  $l = 0, 1, 2$  modes have been evaluated by means of the ADPLS code and compared with the observed ones by requiring an agreement within  $2.5 \mu\text{Hz}$ .

As a result, we find a number of best-fit models corresponding to PMS stars with mass  $3.6\text{--}4.0 M_{\odot}$  and luminosity  $\log L/L_{\odot} \approx 2.1\text{--}2.3$  that reproduce the seven observed periodicities with radial and/or nonradial  $p$  and  $g$  modes. Such

**Table 7.** Preliminary mode identification as a function of the explored model input parameters for models reproducing all seven observed frequencies. The mass is in solar units ( $M_{\odot}$ ) and effective temperature is in K.

Model	$T_{\text{eff}}$	$l$	$f_1$	$f_2$	$f_3$	$f_4$	$f_5$	$f_6$	$f_7$
mod24	3.6	10 402	0	1					
1				-4	-2				2
2			-2	-8	-4	-5	2	0	
mod25	3.7	8 211	0	3		1	6	4	6
1				-2		-1			
2			2	-4	-1	-2	5	3	
mod26	3.7	8 823	0		1		5		
1			1	-3	-1			2	5
2				-5	-2	-3			
mod29	3.8	8 155	0	3		1			
1			2	-2			6	4	6
2			2	-4	0	-1			
mod33	3.9	8 210	0		2				
1			2	-2			6	4	
2				-4	0	-1			6
mod37	4.0	6 997	0	5	1	3	9	9	
1						1		6	
2			4	-2	2	1	8	8	
mod38	4.0	8 253	0		2				7
1			2						
2				-3	0	-1	6	4	6

an independent confirmation of the fundamental stellar parameters range previously estimated for VV Ser is an important by-product of the main objective of asteroseismology (which will be addressed in a future work, requiring more and better observations and more accurate modeling), i.e., of sensing the internal structure of the star. We also notice that if the effective temperature is significantly lower ( $\sim 7000$  K) than the values based on the empirical spectral types ( $\approx 9000$  K), we are able to reproduce all the observed periodicities with  $p$  modes for a stellar mass of  $4 M_{\odot}$  and a luminosity of  $125 L_{\odot}$ . An accurate spectral type determination of VV Ser is urgently needed to discriminate among the different solutions. In the meantime, the present analysis seems to indicate a stellar mass in the range of the largest masses expected (and indeed observed) for this class of pulsators. The possible effect of rotation on the predicted frequencies depends on the adopted estimates of the rotational velocity and inclination angle, as well as on the stellar radius. If the measured periodicity at 2.2 d is interpreted in terms of rotation, the corresponding rotational splitting is of the order of  $m \times 5 \mu\text{Hz}$ . Finally, we note that further photometric observations of VV Ser, especially by means of a multisite campaign, would be of great help to better define the frequency spectrum and to eliminate the uncertainty on the observed frequencies due to the 1 c/d alias.

*Acknowledgements.* We thank the referee, T. Böhm, for useful comments that greatly improved the presentation. V.R. wishes to thank the personnel of the Loiano Observatory for their competent and kind help during the observations. Partial financial support for this work was provided by PRIN-INAF 2005 under the project “Stellar clusters as probes of stellar formation and evolution” (P.I. Francesco Palla). This research has made use of the SIMBAD database operated at CDS, Strasbourg, France. M.J.M. and J.P.M. were supported in part by FCT t

through project POCTI/CTE-AST/57610/2004 from POCTI, with funds from the European programme FEDER.

## References

- Acke, B., & van den Ancker, M. E. 2004, *A&A*, 426, 151  
Alvarez, M., Hernandez, M. M., Michel, E., et al. 1998, *A&A*, 340, 149  
Baglin, A., Barban, C., Goupil, M.-J., Michel, E., & Auvergne, M. 2000, *ASP Conf. Ser.*, 210, 359  
Böhm, T., & Catala, C. 1995, *A&A*, 301, 155  
Böhm, T., Catala, C., Balona, L., & Carter, B. 2004, *A&A*, 427, 907  
Breger, M. 1972, *ApJ*, 171, 539  
Breger, M., Stich, J., Garrido, R., et al. 1993, *A&A*, 271, 482  
Catala, C. 2003, *Ap&SS*, 284, 53  
Catala, C., Donati, J. F., & Böhm, T. 1999, *A&A*, 345, 884  
Chavarría-K., C., de Lara, E., Finkenzeller, U., Mendoza, E. E., & Ocegueda, J. 1988, *A&A*, 197, 151  
Cohen, M., & Kuhl, L. V. 1979, *ApJS*, 41, 743  
D’Antona, F., & Mazzitelli, I. 1994, *ApJS*, 90, 467  
Davis, R., Strom, K. M., & Strom, S. E. 1983, *AJ*, 88, 1644  
de Lara, E., Chavarría-K., C., & Lopez-Molina, G. 1991, *A&A*, 243, 139  
Donati, J.-F., Semel, M., Carter, B. D., Rees, D. E., & Cameron, A. C. 1997, *MNRAS*, 291, 658  
Fernández, M. 1995, *A&AS*, 113, 473  
Fernandez, M., Ortiz, E., Eiroa, C., & Miranda, L. F. 1995, *A&AS*, 114, 439  
Finkenzeller, U. 1985, *A&A*, 151, 340  
Finkenzeller, U., & Mundt, R. 1984, *A&AS*, 55, 109  
Gahm, G. F., Loden, K., Gullbring, E., & Hartstein, D. 1995, *A&A*, 301, 89  
Grady, C. A., Perez, M. R., Talavera, A., et al. 1996, *A&AS*, 120, 157  
Gray, R. O., & Corbally, C. J. 1998, *AJ*, 116, 2530  
Grigahcène, A., Dupret, M.-A., Garrido, R., Gabriel, M., & Scuflaire, R. 2006, *CoAst*, 147, 69  
Herbig, G. H. 1960, *ApJS*, 4, 337  
Hernández, J., Calvet, N., Briceö, C., Hartmann, L., & Berlind, P. 2004, *AJ*, 127, 1682  
Hillenbrand, L. A., Strom, S. E., Vrba, F. J., & Keene, J. 1992, *ApJ*, 397, 613  
Kenyon, S. J., & Hartmann, L. 1995, *ApJS*, 101, 117  
Kurtz, D. W., & Marang, F. 1995, *MNRAS*, 276, 191  
Kuschnig, R., Weiss, W. W., Gruber, R., Bely, P. Y., & Jenkner, H. 1997, *A&A*, 328, 544  
Lenz, P., & Breger, M. 2005, *CoAst*, 146, 53  
Marconi, M., & Palla, F. 1998, *ApJ*, 507, L141  
Marconi, M., Ripepi, V., Alcaà, J. M., Covino, E., Palla, F., & Terranegra, L. 2000, *A&A*, 355, L35  
Marques, J. P., Fernandes, J., & Monteiro, M. J. P. F. G. 2004, *A&A*, 422, 239  
Mora, A., Merín, B., Solano, E., et al. 2001, *A&A*, 378, 116  
Morel, P. 1997, *A&AS*, 124, 597  
Palla, F., & Stahler, S. W. 1993, *ApJ*, 418, 414  
Pinheiro, F. J. G., Folha, D. F. M., Marconi, M., et al. 2003, *A&A*, 399, 271  
Racine, R. 1968, *AJ*, 73, 233  
Reese, D., Lignier, F., & Rieutord, M. 2006, *A&A*, 455, 621  
Ripepi, V., Palla, F., Marconi, M., et al. 2002, *A&A*, 391, 587  
Ripepi, V., Marconi, M., Bernabei, et al. 2003, *A&A*, 408, 1047  
Ripepi, V., Marconi, M., Palla, F., et al. 2006a, *Mem. Soc. Astron. It.*, 77, 317  
Ripepi, V., Bernabei, S., Marconi, M., et al. 2006b, *A&A*, 449, 335  
Rostopchina, A. N., Grinin, V. P., & Shakhovskoi, D. N. 2001, *Astron. Rep.*, 45, 60  
Shevchenko, V. S., Grankin, K. N., Ibragimov, M. A., Mel’Nikov, S. Yu., & Yakubov, S. D. 1993, *Ap&SS*, 202, 121  
Strom, S. E., Grasdalen, G. L., & Strom, K. M. 1974, *ApJ*, 191, 111  
Schmidt-Kaler, Th. 1965, in *Landolt-Börnstein, Numerical data and functional relationship in science and technology, group VI* (Berlin: Springer Verlag), I, 284  
Suran, M., Goupil, M., Baglin, A., Lebreton, Y., & Catala, C. 2001, *A&A*, 372, 233  
Swenson, F. J., Faulkner, J., Rogers, F. J., & Iglesias, C. A. 1994, *ApJ*, 425, 286  
Testi, L., Palla, F., & Natta, A. 1998, *A&AS*, 133, 81  
Vieira, S. L. A., Corradi, W. J. B., Alencar, S. H. P., et al. 2003, *AJ*, 126, 2971  
Weiss, W. W., Aerts, C., Aigrain, S., et al. 2004, *Second Eddington Workshop, ESA SP-538*, 435  
Zwintz, K., Marconi, M., Kallinger, T., & Weiss, W. W. 2004, in *The A star puzzle*, ed. J. Zverko, J. Žižňovský, S. J. Adelman, & W. W. Weiss, *IAU Symp.*, 224, 353



# Online Material

**Table 3.** Log of the observations.

HJD-2 450 000 start (days)	HJD-24 50 000 end (days)	Duration (h)
52 488.362	52 488.517	3.7
52 490.338	52 490.510	4.1
52 492.344	52 492.506	3.9
52 493.335	52 493.490	3.7
52 800.427	52 800.583	3.7
52 801.410	52 801.574	3.9
52 802.425	52 802.578	3.7
52 803.423	52 803.573	3.6
53 182.414	53 182.514	2.4
53 183.371	53 183.482	2.7
53 184.356	53 184.609	6.1
53 185.350	53 185.597	5.9
53 186.420	53 186.600	4.3
53 209.402	53 209.544	3.4
53 210.399	53 210.518	2.9

**Table 5.** Physical properties of the selected PMS models.

Model	Mass $M/M_{\odot}$	Radius $R/R_{\odot}$	Luminosity $L/L_{\odot}$	$T_{\text{eff}}$ K	Age Gy
mod1	2.2	1.99	20.74	8749	5.82
mod2	2.2	1.77	27.27	9913	6.98
mod3	2.4	2.09	29.46	9304	4.65
mod4	2.4	2.04	37.54	10 000	5.11
mod5	2.6	3.54	57.56	8459	3.24
mod6	2.6	3.14	66.90	9319	3.38
mod7	2.6	2.18	43.08	10 023	4.09
mod8	2.8	4.08	66.50	8168	2.63
mod9	2.8	3.23	90.99	9885	2.85
mod10	3.0	4.58	77.3	8007	2.17
mod11	3.0	4.17	91.9	8758	2.17
mod12	3.0	3.74	107.9	9621	2.35
mod13	3.0	3.32	122.2	10 546	2.45
mod14	3.2	4.67	105.7	8573	1.88
mod15	3.2	4.22	125.5	9417	1.96
mod16	3.2	3.75	146.2	10 375	2.04
mod17	3.4	5.37	110.1	8086	1.55
mod18	3.4	4.96	130.4	8762	1.61
mod19	3.4	4.53	152.5	9539	1.67
mod20	3.4	4.08	176.0	10 414	1.73
mod21	3.6	5.71	134.7	8234	1.33
mod22	3.6	5.31	156.4	8869	1.38
mod23	3.6	4.88	180.9	9590	1.43
mod24	3.6	4.44	207.6	10 402	1.48
mod25	3.7	5.95	144.3	8211	1.23
mod26	3.7	5.41	167.0	8823	1.28
mod27	3.7	5.12	192.9	9518	1.32
mod28	3.7	4.68	221.2	10 300	1.36
mod29	3.8	6.21	152.9	8155	1.14
mod30	3.8	5.81	175.9	8727	1.18
mod31	3.8	5.40	202.2	9376	1.22
mod32	3.8	4.97	231.2	10 106	1.26
mod33	3.9	6.39	166.5	8210	1.06
mod34	3.9	6.00	190.7	8766	1.09
mod35	3.9	5.59	218.1	9392	1.13
mod36	3.9	5.16	248.4	10 092	1.16
mod37	4.0	7.63	125.2	6997	0.89
mod38	4.0	6.58	180.5	8253	0.98
mod39	4.0	6.20	205.2	8760	1.02
mod40	4.0	5.80	232.9	9366	1.05
mod41	4.0	5.40	263.8	10 023	1.08

**Table 6.** Preliminary mode identification as a function of the explored model input parameters. The mass is in solar units ( $M_{\odot}$ ) and the effective temperature in K.

Model	Mass	$T_{\text{eff}}$	$l$	$f_1$	$f_2$	$f_3$	$f_4$	$f_5$	$f_6$	$f_7$
Possible value of $n$										
mod1	2.2	8749	0							
			1		-5	-3				
			2							
mod2	2.2	9913	0							
			1			-4	-5			-2
			2	-5	-7	-7	-9			-4
mod3	2.4	9304	0							
			1		-5		-3			
			2		-9	-5	-6			
mod4	2.4	10 000	0							
			1		-6, -7		-4			
			2				-8			-2
mod5	2.6	8459	0							1
			1					1	-1	
			2						-2	
mod6	2.6	9319	0							
			1							
			2						-1	
mod7	2.6	10 023	0							
			1							
mod8	2.8	8168	0	1				3		
			1	-1						2
				-2						2
mod9	2.8	9885	0							
			1							
mod10	3.0	8007	0							4
			1		-4		-2			
			2	-1	-7		-4	3		
mod11	3.0	8758	0	1				3		
			1	-1	-5	-2				2
			2	-2	-8, -9		-5			2
mod12	3.0	9621	0							
			1		-6					
			2	-3	-10	-5	-6			
mod13	3.0	10 547	0							
			1		-6	-3	-4			
			2	-4	-11	-6	-7			
mod14	3.2	8573	0							4
			1		-4		-2			
			2	-1	-7	-3	-4	3		
mod15	3.2	9417	0	1	-5			3		
			1	-1	-9	-2				2
			2	2	-8	-4	-5			2
mod16	3.2	10 375	0							1
			1		-5			1		
			2	-3	-10	-5	-6			
mod17	3.4	8086	0			1		5		
			1	1	-3	-1				2
			2		-5	-2	-3			
mod18	3.4	8762	0							
			1		-3			4		4
			2		-6, -7	-3	-4			
mod19	3.4	9538	0							2
			1		-4					1
			2		-7, -8					
mod20	3.4	10 414	0							
			1		-5		-3			
			2		-9			1	-1	
mod21	3.6	8234	0							
			1				-1	5		
			2	1	-5	-1	-2			3

**Table 6.** continued.

Model			$f_1$	$f_2$	$f_3$	$f_4$	$f_5$	$f_6$	$f_7$
Mass	$T_{\text{eff}}$	$l$	Possible value of $n$						
mod22		0	2					3	5
3.6	8868	1	1	-3	-1				
		2		-6	-2	-3		2	4
mod23		0					4		4
3.6	9590	1			-2				
		2		-7	-3	-4	3	1	
mod24		0	1						
3.6	10402	1		-4	-2				2
		2	-2	-8	-4	-5	2	0	
mod25		0	3			1	6	4	6
3.7	8211	1		-2		-1			
		2	2	-4	-1	-2	5	3	
mod26		0			1		5		
3.7	8823	1	1	-3	-1			2	5
		2		-5	-2	-3			
mod27		0							
3.7	9518	1		-3			4		
		2	0	-6					
mod28		0							2
3.7	10300	1		-4		-2		1	
		2	-1	-7, -8		-4			
mod29		0	3			1			
3.8	8155	1	2	-2			6	4	6
		2	2	-4	0	-1			
mod30		0							
3.8	8727	1				-1	5		
		2	1	-5	-1	-2		3	
mod31		0	2	-3				3	5
3.8	9376	1	1	-6	-1				
		2		-5	-2	-3		2	4
mod32		0					4		4
3.8	10106	1				-2			
		2		-7	-3	-4	3	1	
mod33		0			2				
3.9	8210	1	2	-2			6	4	
		2		-4	0	-1			6
mod34		0				0		4	6
3.9	8766	1		-2		-1			
		2		-4	-1	-2	5	3	5
mod35		0			1		5		
3.9	9392	1	1	-3	-1			2	
		2		-5	-2	-3	4		
mod36		0							
3.9	10092	1		-3					4
		2	0	-6					
mod37		0	5	1	3		9		9
4.0	6997	1				1		6	
		2	4	-2	2	1	8		8
mod38		0			2				7
4.0	8253	1	2						
		2		-3	0	-1	6	4	6
mod39		0	3			1	6	4	
4.0	8760	1		-2					6
		2	2	-4		-1			
mod40		0			1				
4.0	9366	1				-1	5		5
		2	1	-5	-1	-2			
mod41		0	2					3	
4.0	10023	1		-3	-1				
		2	0	-6	-2	-3		2	4